Environmental Science Nano

Colloidal Stabilization of Hydrophobic InSe 2D Nanosheets in a Model Environmental Aqueous Solution and their Impact on Shewanella oneidensis MR-1

Journal:	*Environmental Science: Nano*
Manuscript ID	EN-ART-06-2023-000382.R2
Article Type:	Paper

Colloidal Stabilization of Hydrophobic InSe 2D Nanosheets in a Model Environmental Aqueous Solution and their Impact on *Shewanella oneidensis* MR-1

Shreyasi Sengupta[a], Swapnil B. Ambade[a], Tana L. O'Keefe[b], Falak Tawakalna[c], Jenny K. Hedlund Orbeck[d], Robert J. Hamers[d], Z. Vivian Feng[c,e], Christy L. Haynes[b], and Zeev Rosenzweig[a]*

[a]Department of Chemistry and Biochemistry, University of Maryland Baltimore County, Baltimore, MD 21250, United States

[b]Department of Chemistry, University of Minnesota, 207 Pleasant Street SE, Minneapolis, Minnesota 55455, United States

[c]Chemistry Department, Augsburg University, Minneapolis, Minnesota 55454, United States

[d]Department of Chemistry, University of Wisconsin Madison, Madison, Wisconsin 53706, United States

[e]Council on Science and Technology, Princeton University, Princeton, NJ 08544, United States

Environmental Significance

Despite the rapid proliferation of their applications, there have been a limited number of studies to assess the impact of emerging 2D materials on the environment. The current study focuses on a seemingly non-hazardous 2D material composed of indium selenide (InSe). InSe 2D material has gained recent popularity due to its high photoresponsivity and suitability as a component of wearable and flexible electronics. InSe nanosheets are highly hydrophobic and do not disperse nor dissolve to ionic species in aqueous media. Even if the nanosheets were to dissolve, the expected ions of indium and selenium are not considered highly toxic. As a direct bandgap semiconducting material, reactive oxygen species (ROS) generation is a possibility, yet our results do not support significant levels of ROS generation from InSe nanosheets when exposed to ambient light. With no obvious degradation pathway and a high level of hydrophobicity, it would be reasonable to expect that InSe nanosheets would aggregate and settle in aqueous media and remain in the soil. And yet, this study reveals that the hydrophobic InSe nanosheets are colloidally stable in aqueous solutions that contain epigallocatechin gallate (EGCG), a natural organic matter (NOM) simulant. Coating the hydrophobic InSe nanosheets with EGCG renders them colloidally stable in water and enables their interactions with bacterial organisms in the solution. We found that the impact of the colloidally stable InSe-EGCG nanosheets on bacterial growth is driven by the EGCG molecules either when adsorbed to the surface of the nanosheets and/or desorbed from the surface. InSe-EGCG nanosheets show measurable but relatively low impact on bacterial growth compared to other semiconducting nanomaterials like CdSe quantum dots but the study raises a concern that similar colloidal stabilization processes of seemingly non-toxic hydrophobic materials with limited biodegradation rates could occur in aqueous media due to interactions of the hydrophobic materials with persisting amphiphilic ligands. The resulting colloidally stable materials could adversely impact microorganisms when dispersed in aqueous systems.

ABSTRACT

Semiconductor InSe 2D nanomaterials have emerged as potential photoresponsive materials for broadly distributed photodetectors and wearable electronics technologies due to their high photoresponsivity and thermal stability. This paper addresses an environmental concern about the fate of InSe 2D nanosheets when disposed and released into the environment after use. Semiconducting materials are potentially reactive and often form environmentally damaging species, for example reactive oxygen and nitrogen species, when degraded. InSe nanosheets are prepared using a semi bottom-up approach which involves a reaction between indium and selenium precursors at elevated temperature in an oxygen-free environment to prevent oxidation. InSe nanosheets are formed as a stable intermediate with micrometer-sized lateral dimensions and a few monolayer thickness. The InSe 2D nanosheets are obtained when the reaction is stopped after 30 minutes by cooling. Keeping the reaction at elevated temperature for a longer period, for example 60 minutes leads to the formation of InSe 3D nanoparticles of about 5 nm in diameter, a thermodynamically more stable form of InSe. The paper focuses on the colloidal stabilization of InSe nanosheets in an aqueous solution that contains epigallocatechin gallate (EGCG), a natural organic matter (NOM) simulant. We show that EGCG coats the surface of the hydrophobic, water-insoluble InSe nanosheets via physisorption. The formed EGCG-coated InSe nanosheets are colloidally stable in aqueous solution. While unmodified semiconducting InSe nanosheets could produce reactive oxygen species (ROS) when illuminated, our study shows low levels of ROS generation by EGCG-coated InSe nanosheets under ambient light, which might be attributed to ROS quenching by EGCG. Growth-based viability (GBV) assays show that the colloidally stable EGCG-coated InSe nanosheets adversely impact the bacterial growth of *Shewanella oneidensis* MR-1, an environmentally relevant Gram-negative bacterium in aqueous media. The impact on bacterial growth is driven by the EGCG coating of the nanosheets. In addition, live/dead assays show insignificant membrane damage of the *Shewanella oneidensis* MR-1 cells by InSe nanosheets, suggesting a weak association of EGCG-coated nanosheets with the cells. It is likely that the adverse impact of EGCG-coated nanosheets on bacterial growth is the result of increasing local concentration of EGCG either when adsorbed on the nanosheets when the nanosheets interact with the cells, or when desorbed from the EGCG-coated nanosheets to interact with the bacterial cells.

INTRODUCTION

Two-dimensional (2D) materials are solid, layered nanostructures with strong in-plane chemical bonds but weak out-of-plane van der Waals interactions, with thickness ranging from 1 to 100 nm.[1, 2] Examples of 2D materials include layered (including monolayer) carbons, chalcogenides, and silicate minerals. 2D materials have been shown to possess unique thermal, electronic, electrical, optical, physiochemical, elastic, and mechanical properties, many of which are temperature, bandgap, atmosphere, and material dependent.[3-5] These high aspect ratio sheet-like solids have high surface areas, and with their wide array of chemical compositions, crystal phases, physical forms, and electronic properties, they enable a host of future technologies in areas that include electronics, sensors, catalysis, coatings, barriers, energy storage and conversion, wearable electronics, and biomedicine.[1, 6, 7] With the emergence of 2D nanomaterials in broadly distributed technologies, an effort has begun to understand their biological and environmental interactions and to assess their environmental and human health impact.[1] A specific concern has been raised about the environmental impact of semiconductor 2D materials due to their tendency to generate reactive oxygen species (ROS) when illuminated with sunlight.[8, 9] For example, MoS_2 and Sb_2Se_3 nanosheets were reported to exhibit antibacterial activity on *E. Coli* and *S. aureus* bacteria, but the mechanism of their impact is not fully understood.[10, 11] Another study revealed that industrial grade MoS_2 nanosheets induce cellular uptake, cytotoxicity and inflammation.[12]

This study focuses on InSe, an emerging type of III-VI semiconductor 2D material. In a 2D geometry, InSe is a direct band gap semiconductor with a bandgap of 1.95 eV.[13] The bandgap is highly tunable, enhancing the material's photoluminescent properties. [14, 15] Due to its high photoresponsivity and mechanical flexibility, thin films composed of InSe 2D nanosheets have emerged as materials of interest in flexible and wearable electronics.[16-18] Therefore, a broad distribution of InSe and similar 2D materials in the environment due to their utility in wearable electronics and flexible electronic devices is likely.[16, 19] The chemical composition of InSe nanosheets makes them unlikely to pose a significant environmental concern as both indium and selenium are not considered highly toxic.[16] However, the unique morphology of InSe 2D materials, which could potentially expose bacterial cells to sharp edges, and their high surface area and potential reactivity could lead to strong interactions and adverse impact on microorganisms in the environment. It is important to note that there have not been any studies

on the impact of InSe nanosheets and similar direct gap semiconductor 2D materials on organisms in the environment.

As-synthesized, InSe nanosheets aggregate and settle in aqueous solution due to their high hydrophobicity. As a result, their ability to impact organisms in an aqueous environment is rather limited. However, colloidal stabilization of the hydrophobic InSe nanosheets by natural organic matter (NOM) when released to the environment is possible as was previously shown for graphene and graphene oxide 2D materials.[20] In our experiments, we exposed the InSe nanosheets to epigallocatechin gallate (EGCG), an amphiphilic molecule, which was previously used as a NOM simulant.[21] We exposed the InSe nanosheets to EGCG and measured the impact of EGCG-coated InSe nanosheets on the growth of *Shewanella oneidensis* MR-1 bacterial cells. *Shewanella oneidensis* MR-1 is an environmentally relevant Gram-negative bacterium. It is often used as a model organism for bioremediation research due to its metal-reducing capabilities.[22] Thus, this study focuses on revealing the mechanism of interaction between EGCG-coated InSe nanosheets and bacterial cells.

EXPERIMENTAL METHODS

Materials and Reagents - Indium chloride ($InCl_3$), selenium powder (Se), oleylamine, ethanol, 95% pure epigallocatechin gallate (EGCG, a natural organic matter simulant), NaCl, HEPES and KNO_3 were purchased from Sigma Aldrich. Hydrogen peroxide (H_2O_2) and the fluorescent probes dichlorodihydrofluorescein diacetate (H_2DCFDA) and Amplex Red were purchased from Thermo Fischer. *Shewanella oneidensis* MR-1 BAA1096 and 106686 were purchased from ATCC. BD™ Difco™ Dehydrated Luria-Bertani (LB) broth and agar were purchased from BD Difco (Franklin Lakes, NJ). 1X Dulbecco's phosphate-buffered saline without Ca and Mg was purchased from Corning (Aurora, CO). Millipore deionized water was used without further treatment. All reagents were used as received without further purification.

Synthesis of InSe Nanosheets and Nanoparticles - InSe nanosheets samples of about 200 mg were synthesized following a previously reported semi bottom-up approach.[23] $InCl_3$ and Se powder were used as the respective precursors, and oleylamine (OLA) was used as the solvent, surfactant, and reducing agent. 0.395 g (5 mmol) of $InCl_3$ and 1.106 g (5 mmol) of Se powder were placed into a 50 ml three-neck flask. 10 mL of OLA was then added in as a solvent, surfactant, and reductant to reduce selenium. The mixture was heated rapidly to 200℃ under nitrogen atmosphere and vigorous magnetic stirring. During the heating process, the mixture, which appeared to be homogenous, changed its color from black to yellow and to dark brown when a temperature of 200℃ was attained. At this temperature, aliquots were collected at 30 minutes (InSe nanosheets) and 60 minutes (InSe nanoparticles) and then allowed to cool to room temperature. The samples were washed with ethanol via five repeated cycles of 10-minute-long centrifugation at 5000 rpm and resuspended in ethanol. The samples were then dried at room temperature for 12 h to obtain dark brown powders. The synthesis forms InSe nanomaterials of different size and morphology, which are isolated at different time intervals.

Adsorption of EGCG onto InSe Nanosheets and Nanoparticles - 5 mg InSe nanosheets and nanoparticles were separately added to 1 ml 5 mM EGCG in DI water solution in a 5 ml glass vial. The mixture was stirred at room temperature for 24 hours. The resultant dark solution formed in the process was transferred to another vial using a pipette to obtain a transparent solution of InSe-EGCG in water, leaving behind settled non-dispersible aggregates.

Characterization of Unmodified and EGCG-coated InSe Nanosheets - The UV-vis spectra of unmodified and surface-modified InSe nanosheets were measured using an Agilent Cary 3500 UV-vis multicell peltier spectrophotometer. Background subtracted UV-vis spectra of unmodified InSe nanosheets suspended in ethanol, and surface-modified InSe nanosheets suspended in DI water were measured in a 1 cm quartz cuvette. Zeta potential measurements were carried out using a Malvern Nano Zetasizer ZEN3600 instrument. Unmodified and surface-modified samples of InSe nanosheets were placed in disposable folded capillary cells. Transmission electron microscopy (TEM) images were obtained using a 100 kV FEI Morgagni 268 TEM instrument with 0.1 nm resolution, equipped with a Gatan Orius CCD camera with 250K magnification. The samples were prepared by placing a drop of the suspended unmodified and surface-modified InSe nanosheets onto carbon-copper grids. The samples were then allowed to dry at room temperature overnight. X-ray photoelectron spectroscopy (XPS) measurements were conducted using a PHI VersaProbe III (Physical Electronics, Inc.) equipped with an Al Kα source (1486.6 eV). Measurements were acquired with dual-beam charge neutralization which utilizes a low energy argon ion beam and electron flood gun. Spectra were calibrated to adventitious carbon at 284.8 eV. For inductively coupled plasma mass spectrometry (ICP-MS) measurements, an external calibration curve was created using the Multi-Element Calibration Standard 3 from PerkinElmer. For this, calibration points of 10, 25, 50, 100, 200, 300 ppb were made by serial dilution using DI water as the diluent. In-115 and Se-77 were analyzed using a PerkinElmer NexION 300D ICP mass spectrometer, equipped with a PerkinElmer S10 autosampler. Calibration standards were run prior to samples, with two blank runs of DI water between the standards and samples. The analysis method included 40 sweeps per reading with one reading per replicate. All sample analysis was conducted in triplicate and averaged.

Detection of Reactive Oxygen Species (ROS) and H_2O_2 - To probe ROS formation as a toxicity mechanism, we employed an amperometric method to detect the presence of hydrogen peroxide (H_2O_2), the most stable form of ROS, in the EGCG-InSe suspension using 4-mm commercial DropSens Prussian Blue/carbon screen-printed electrodes under conditions of ambient light. The electrochemical experiment was set up with the printed carbon auxiliary electrode and an external Ag/AgCl reference electrode. Amperometric measurements were set to monitor the current signals at -0.23 V vs. Ag/AgCl reference electrode in 0.1 M KNO_3 supporting electrolyte. Measurements were conducted in 20 ml glass vials. A 5 mM EGCG

solution was used to monitor the background signal. A solution containing 15 μM H_2O_2 and 5 mM EGCG was used as a positive control. A solution containing 500 mg/L InSe nanosheets and 5 mM EGCG was used to detect H_2O_2 formation. To verify the impact of EGCG on H_2O_2 formation near InSe nanosheets, experiments were also conducted by suspending unmodified InSe nanosheets in 0.1 M KNO_3. However, due to the highly hydrophobic nature of the nanosheets, InSe nanosheets were unevenly distributed in the stirred electrochemical cell.

Bacterial Growth-Based Viability Assay - The growth-based viability (GBV) assay procedure and data processing have been described in detail elsewhere.[24] Briefly, *Shewanella oneidensis* MR-1 BAA1096 was stored at -80°C until ready for use. The bacterial stock was plated on a sterilized Luria-Bertani (LB) agar plate and incubated at 30°C overnight. The resulting bacterial colonies were inoculated in 10 mL of LB media and incubated in an orbital shaker at 30°C for 4-6 hours or until the mid-log phase (OD_{600}~0.5). Next, the culture was centrifuged at 750 x *g* for 10 minutes, resuspended with 1X Dulbecco's phosphate-buffered saline (DPBS), and centrifuged again at 750 x *g* for 10 minutes. The pellet was resuspended in HEPES buffer (2 mM HEPES, 25 mM NaCl, pH=7.4) to obtain an optical density of 0.1 at 600 nm. In a 96-well plate, bacteria were exposed to the EGCG-coated InSe nanosheets (InSe-EGCG) at concentrations ranging from 1.95 to 1000 mg/L for 1 h. After the exposure, a 5 μL of each suspension was removed and added to 195 μL of fresh LB broth in a new 96-well plate in triplicate. Optical density at 600 nm was measured with a BioTek Synergy™ 2 multi-mode microplate reader every 20 minutes over the course of 15 h at 30°C with medium-intensity shaking for 30 seconds prior to each reading. The collected growth curves were analysed using the R packages provided by Qui et al. to provide the bacterial viability post-exposure.[24] Bacterial growth curves in the presence of thoroughly washed InSe-EGCG nanosheets at varying concentrations were performed on *Shewanella oneidensis* MR-1 106686. The bacterial growth conditions were similar to the ones described above. The optical density of bacterial solutions at 600 nm was measured as a function of time using a Molecular Devices Versamax Absorbance Microplate Reader. We assume that the two strains of *Shewanella oneidensis* MR-1 respond similarly to the presence of InSe-EGCG nanosheets under similar conditions.

Live/Dead Assay - The Live/Dead BacLight Bacterial Viability kit (ThermoFisher Scientific) was used to assess bacterial membrane damage by EGCG InSe 2D nanomaterials. *Shewanella oneidensis* MR-1 was exposed to EGCG-coated InSe concentrations of 0, 1.95, 7.81, and 62.5 mg/L for 1 h. Then, samples were distributed to a 96-well plate and were exposed to a stain containing a mixture of green-fluorescent SYTO 9 and red-fluorescent propidium iodide (PI) dyes for 15 min, following the manufacturer's recommendations. Fluorescence measurements were obtained using a Tecan Spark plate reader with an excitation wavelength of 485 nm and emission at 528 nm and 638 nm for SYTO 9 and propidium iodide, respectively. The fluorescence intensity ratio of SYTO 9 to PI was determined for each exposure concentration and normalized to that of a negative control bacterial sample not exposed to EGCG-coated InSe. Cell-permeant SYTO 9 stains all live cells, while the non-permeant PI stains nucleic acids only in the cells with damaged membranes.[25]

RESULTS AND DISCUSSION

Synthesis and Characterization of InSe Nanosheets and Nanoparticles - Previous studies have often utilized exfoliation methods to prepare 2D materials including InSe.[2,26-28] Exfoliation methods involve forming nanosheets from a bulk layered material by breaking the van der Waals interactions between the layers.[2, 26-28] While successful in forming high-quality 2D materials, it is challenging to form 2D materials of sufficient quantities for environmental exposure studies using exfoliation methods alone. To overcome this challenge, we adopted a semi bottom-up approach, recently reported by Moloto and co-workers to prepare InSe nanosheets to study the impact of InSe nanosheets on bacterial organisms.[23] The semi bottom-up approach is similar to the hot injection method used to form semiconductor quantum dots.[29] The synthesis of InSe nanosheets and their coating and colloidal stabilization in aqueous solution with EGCG, which are described in the following sections, are shown in Scheme 1.

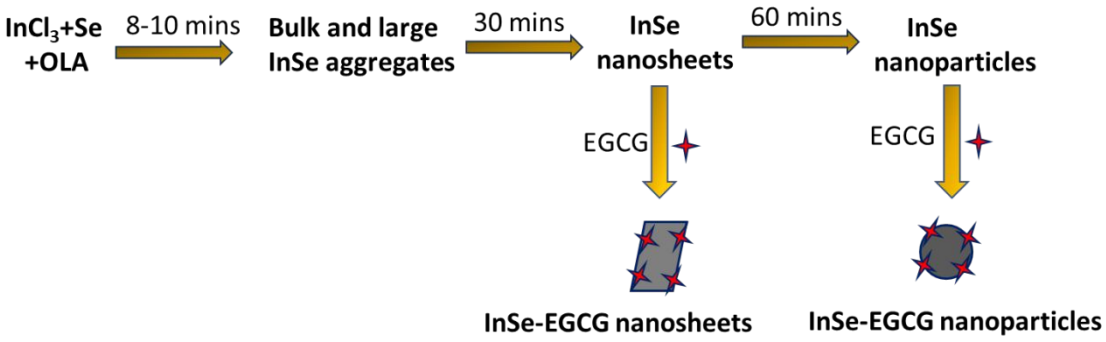

Scheme 1 – Synthesis of InSe nanosheets and nanoparticles and their coating and colloidal stabilization in aqueous solution with EGCG

The reaction starts with the dissolution of the precursors at elevated temperature of 200°C. A rapid nucleation of oppositely charged ions and growth follows. These processes result in the formation of a heterogeneous sample of bulk InSe which then self-digest to form InSe nanosheets and later mono-dispersed InSe nanoparticles, which are thermodynamically more stable. Under our experimental conditions, InSe nanosheets of various lateral dimensions but with consistently a few monolayers thickness are formed after 30 minutes. The formed nanosheets break down to nanoparticles due to high lateral strain. InSe nanoparticles are formed after 60 minutes. Our results are in agreement with previous studies that utilized

detailed TEM measurements to follow the formation of InSe nanosheets and nanoparticles using this approach.[23] It must be noted however, that additional studies are needed to better understand the mechanism of the formation of InSe nanosheets and nanoparticles using this semi bottom-up approach. The semi bottom-up synthesis approach is highly versatile. Using this approach, InSe 2D materials can be formed in different crystalline phases (α, β, γ), stoichiometries, and oxidation states depending on the precursors used and the reaction conditions[13,30,31] InSe 2D nanosheets of different lattice constants show different band gap values.[13] Structural modification and band-gap crossover in InSe nanosheets have also been previously reported.[32]

Figure 1 summarizes the characterization of InSe nanosheets synthesized using the method described in scheme 1. Figure 1a shows a representative photo of a 20 mg sample of InSe nanosheets powder. Figure 1b shows the normalized UV-vis absorbance spectra of the as-synthesized InSe nanosheets (30 minutes, blue) and nanoparticles (60 minutes, red) in toluene. The UV spectral features and especially the observed red shift as the InSe nanosheets form are in agreement with previous studies.[23] Figure 1c and 1d show TEM images of InSe nanosheets and nanoparticles, respectively. The micrometric lateral dimensions and lower thickness of the InSe nanosheets are easily observed in Figure 1C. The presence of 3-5 nm InSe nanoparticles in Figure 1D confirms the ability to kinetically control the size and morphology of the InSe nanosheets or nanoparticles using this semi bottom-up method.

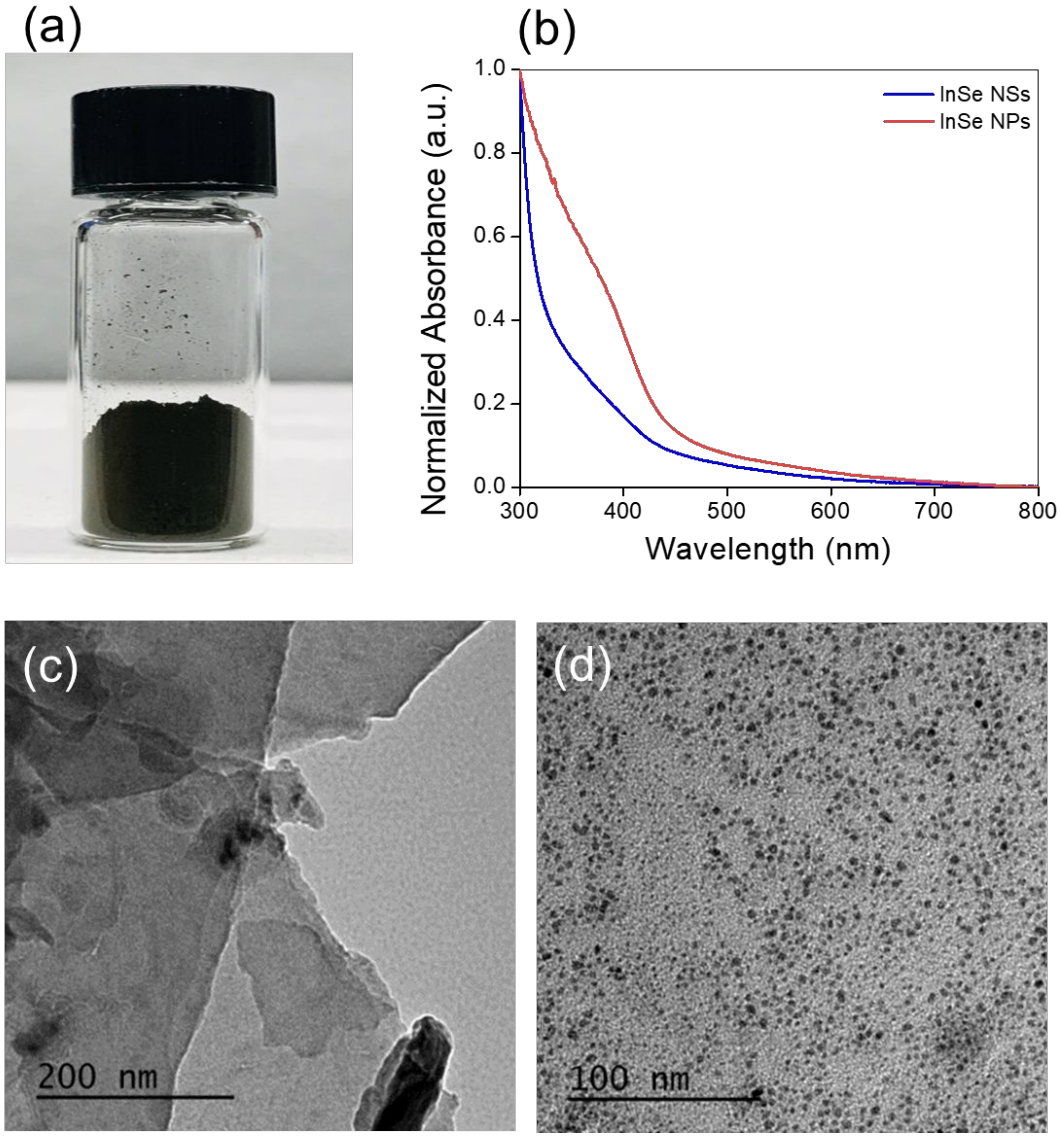

Figure 1- (a) Vial image of scalable InSe nanosheets powder; (b) Normalized UV-vis spectra of InSe nanosheets (30 minutes, blue) and nanoparticles (60 minutes, red) in toluene; (c) TEM images of InSe nanosheets (left) and (d) nanoparticles (right) synthesized by a semi bottom-up method.

Figure 2 shows representative XPS data collected on the InSe nanosheets. The high-resolution elemental regions for In(3d) and Se(3d) were evaluated. The maxima observed at binding energy values of 452.0 and 444.5 eVs are indicative of the In $3d_{3/2}$ and $3d_{5/2}$ peaks respectively and confirm the presence of In^{3+} mainly in the form of In_2Se_3 with some oxidation to In_2O_3.[33, 34] The binding energy value of 54.7 eV contains overlapping Se $3d_{5/2}$ and $3d_{3/2}$ peaks that are not resolved given the small difference in the energy splitting of these peaks. Nevertheless, the location of this peak is indicative of Se^{-2} in the form of In_2Se_3 and the smaller peak at 59.1 eV indicates the presence of minor oxidation to SeO_2. Overall, the XPS results confirm the elemental composition and oxidation states of InSe in these materials with no significant contaminants.

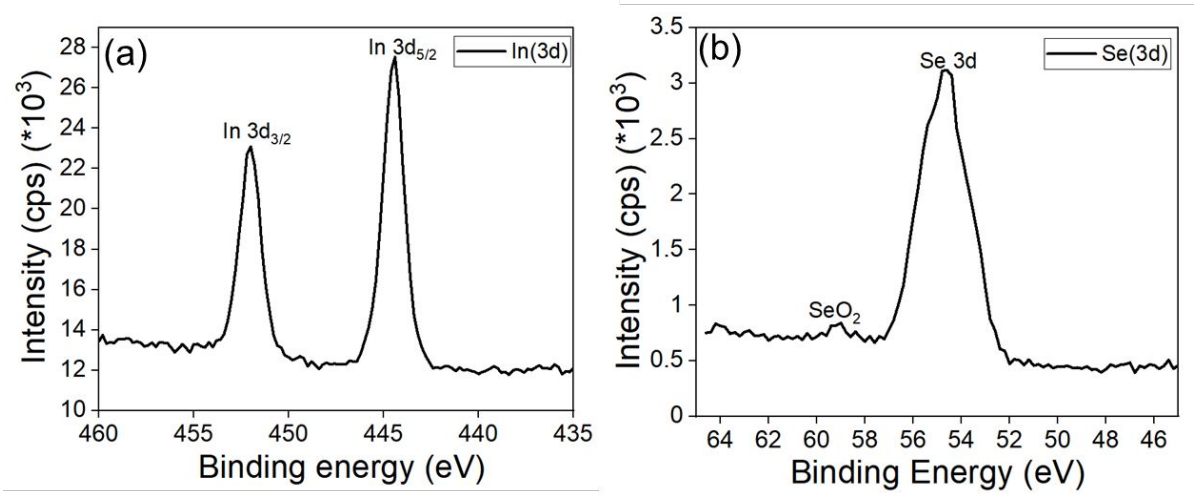

Figure 2 – High resolution XPS data analysis of InSe nanosheets including (a) In(3d) and (b) Se(3d) regions. The results indicate high purity with In_2Se_3 as the dominant composition and negligible oxidation to In_2O_3 and SeO_2.

Synthesis and Characterization of EGCG-coated InSe Nanosheets - As previously mentioned, InSe 2D nanosheets are hydrophobic and not soluble in aqueous media. The hydrophobic InSe surface enables strong physisorption of amphiphilic molecules like the NOM simulant epigallocatechin gallate (EGCG), which shows some antimicrobial properties as well.[35, 36] Figure 3a shows the chemical structure of EGCG, and figure 3b shows a transparent aggregation-free solution of InSe nanosheets following their coating with EGCG in DI water. In contrast, figure 3c shows a photo of a DI water solution following the addition of 3 mg unmodified InSe nanosheet powder. The solution is colorless, and dark-colored InSe nanosheets are seen floating at the top of the solution. It is clear that the InSe nanosheets are insoluble in water in the absence of the EGCG coating. Figure 3d shows the normalized UV-vis spectra of EGCG-coated InSe nanosheets at increasing concentrations in DI water. The absorbance at around 400 nm is indicative of EGCG-coated InSe nanosheets.[23] Figure 3e shows a representative TEM image of EGCG-coated InSe nanosheets with lateral dimensions of 200-250 nm. The additional black features in the image compared to the TEM image in Figure 1c are attributed to the presence of EGCG. Importantly, the TEM and UV-vis results described in Figure 3d and 3e show that the InSe nanosheets are colloidally stable in aqueous solution due to the formation of EGCG coating on the nanosheets' surface but remain intact.

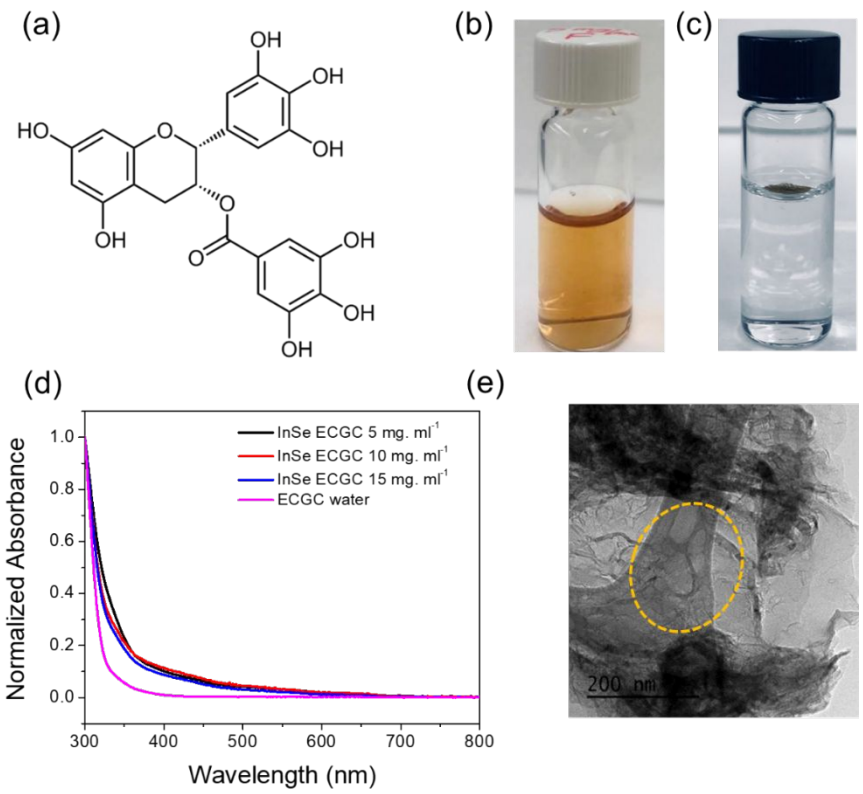

Figure 3 - (a) EGCG chemical structure; (b) InSe-EGCG and (c) Hydrophobic InSe nanosheet powder in water solutions; (d) Normalized UV-vis spectra of InSe-EGCG water at different concentrations (black, red, and blue) and EGCG in water (pink) as the reference and (e) TEM image of EGCG coated InSe nanosheets in water. These measurements confirm the presence of the EGCG coating on the surface of the InSe nanosheets which renders them colloidally stable.

Interestingly, the EGCG-coated InSe nanosheets in phosphate buffer solution show a negative zeta potential of -12 mV while it is near 0 in DI water. This low negative surface charge is most likely due to the adsorption of phosphate ions, which are in excess in a phosphate buffer solution on the surface. EGCG itself has multiple hydroxyl groups but no net surface charge. The colloidal stabilization of the InSe-EGCG nanosheets might be attributed to the formation of hydrogen bonds between the hydroxyl groups of EGCG and water molecules. It should also be noted that zeta potential measurements which are carried out on DLS instruments with zeta potential measurement capabilities provide accurate zeta potential values of nanospheres but not of nanosheets. While these measurements provide accurate information about the net surface charge, positive or negative, the measured absolute zeta potential values may not be accurate. Figures S1 and S2 show the dynamic light scattering (DLS) size measurements and scanning electron microscopy with energy dispersive X-ray analysis (SEM-EDX) spectra

respectively, of unmodified InSe nanosheets and EGCG-coated InSe nanosheets. Previous studies have shown that unmodified InSe nanosheets are prone to surface oxidation.[28, 37] UV-vis spectra of EGCG-coated InSe nanosheets over several days show no significant change. This suggests that surface modification with molecules like EGCG increases the chemical stability of InSe nanosheets towards oxidation.

Colloidal Stabilization of InSe Nanosheets in Aqueous Solution with EGCG - To find out the ratio between EGCG and InSe nanosheet concentrations that maximizes the colloidal stabilization of InSe nanosheets in aqueous solution, a fixed concentration of InSe nanosheets (1mg/ml) was coated with EGCG in aqueous solutions of varying EGCG concentrations (0-3 mM). The absorption intensity at 375 nm (a characteristic peak of InSe nanosheets) was used to quantify the colloidal stabilization efficiency of the InSe-EGCG nanosheets. ICP-MS measurements were also used to quantify the level of indium (In-115) and selenium (Se-77) in the InSe-EGCG nanosheets that were formed in the EGCG solutions at all EGCG concentrations. Given the high sensitivity of ICP-MS measurements, the InSe-EGCG solutions were diluted 100-fold in DI water to obtain the ICP-MS data. Figure 4a shows the InSe nanosheets (1mg/ml) absorbance at 375 nm at varying EGCG concentrations and Figure 4b shows the ICP-MS signals of indium and selenium in the InSe-EGCG nanosheets (1mg/ml) formed at varying EGCG concentrations. Both the InSe UV-vis absorbance and ICP-MS measurements confirm that the colloidal stabilization of InSe nanosheets in water is near 0 in the absence of EGCG. This condition serves as a negative control. The UV-vis and ICP-MS measurements also show that the colloidal stabilization efficiency of 1 mg/ml InSe-EGCG nanosheets reaches a plateau at EGCG concentrations greater than 0.75 mM. Varying the pH of the solutions did not significantly change the concentration of EGCG-InSe nanosheets in the solution (data not shown). This suggests that the colloidal stabilization of InSe nanosheets by EGCG is driven by hydrophobic interactions between the EGCG backbone and the hydrophobic InSe surface, and that the strength of these interactions depends mostly on the ratio between the concentrations of EGCG and InSe nanosheets and not on the solution pH.

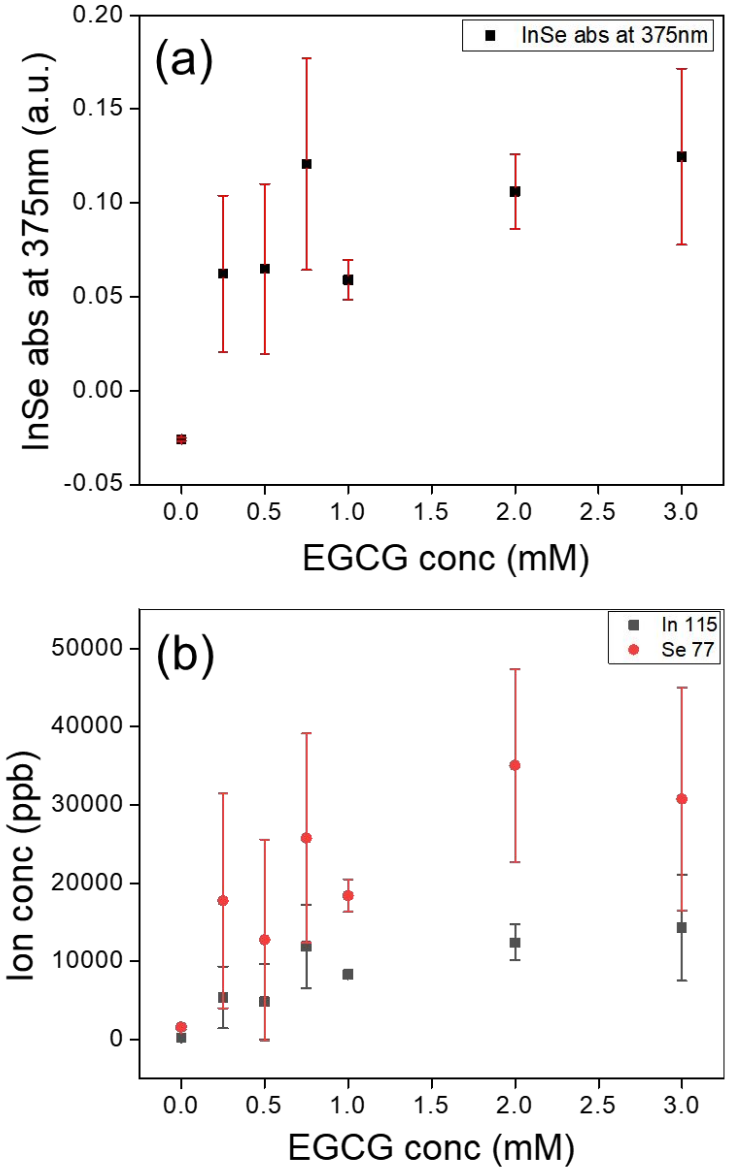

Figure 4 – (a) UV-vis absorbance at 375 nm and (b) ICP-MS results of In-115 and Se-77 ions concentrations from InSe nanosheets (1mg/ml) at varying EGCG concentrations at pH 7.0. All the data were obtained in triplicate samples and averaged.

Reactive Oxygen Species (ROS) Generation – We conducted experiments to determine whether reactive oxygen species (ROS) are generated by EGCG-coated InSe nanosheets when exposed to ambient light. We utilized an amperometric method to detect H_2O_2, the most stable form of ROS. We note that, due to optical interference and quenching reactions between EGCG and fluorescence probes (both DCFDA and Amplex Red), detection of H_2O_2 using fluorescence dye-based methods were proven unsuccessful. Amperometric measurements of H_2O_2 were conducted with a screen-printed Prussian Blue/Carbon electrode. The limit of detection for hydrogen peroxide of this amperometric method was found to be 4.1 μM. While generally less sensitive than fluorescence techniques, this amperometric method was used successfully to detect micromolar levels of H_2O_2 formed due to the REDOX transformations of lithium cobalt oxide (LCO) battery materials.[38, 39] In our experiments, adding H_2O_2 to a final concentration of 15 μM in 5 mM EGCG solution increased the current compared to the background current signal when the electrode was immersed in a 5 mM EGCG solution by about 50%. This signal increase indicated that the amperometric detection method was sensitive to the presence of H_2O_2 in the solution. However, we did not observe a current change when the electrode was immersed in a solution containing InSe-EGCG nanosheets when compared to the EGCG background current. These results suggest that InSe-EGCG nanosheets, even at high levels of 250 mg/L do not form H_2O_2 levels above the 4.1 μM limit of detection of our amperometric method. This contrasts with the 10-15 μM levels of H_2O_2 formed when LCO at 10-fold lower concentrations undergo redox transformations in aqueous solution.[38, 39] This surprising low level of ROS generation by a semiconducting material with bandgap of 1.95 eV might be attributed to reduced interactions between the ROS active semiconducting surface and water or oxygen molecules in the solution by the EGCG coating, and/or because the EGCG coating quenches any formed ROS. The amperometric measurements with unmodified InSe nanosheets (without EGCG in solution) also did not suggest the presence of significant H_2O_2 when suspended in a 0.1M KNO_3 solution, possibly due to the nanosheets' aggregation.

Antibacterial Effect of InSe nanosheets on *Shewanella oneidensis* MR1- Despite the fact that InSe nanosheets do not dissolve to produce toxic ions and do not generate measurable levels of ROS when coated with EGCG, our experiments revealed that they affect bacterial growth. We carried out growth-based viability (GBV) studies and membrane viability studies to better understand the impact of InSe-EGCG nanosheets on *Shewanella oneidensis* MR-1. We first conducted GBV experiments by exposing the bacterial cells to increasing concentrations of InSe-EGCG nanosheets and nanoparticles in 5 mM EGCG solutions. In these experiments, the bacterial cells were exposed to the same EGCG level, and the only difference was the ratio between adsorbed and free EGCG molecules in the solution. Figure 5a shows the normalized growth-based viability (GBV) assay results of *Shewanella oneidensis* MR-1 when exposed to InSe-EGCG nanosheets or nanoparticles (0-1000 mg/L) while keeping the EGCG concentration constant at 5 mM. Both the InSe nanosheets and nanoparticles are seen to have minimal or no added toxicity on *Shewanella oneidensis* MR-1 at all concentrations beyond the toxicity of free EGCG. Free EGCG at 5 mM reduces the viability of *Shewanella oneidensis* MR-1 to 20% compared to a negative control when the bacterial cells are grown in an EGCG-free and InSe-EGCG-free LB growth media. Adding InSe nanosheets to the solution does not affect this level of toxicity regardless of InSe shape or concentration. Fluorescence-based live/dead assays were performed to quantify membrane damage and understand potential impacts of membrane association.[25] This fluorescence-based method uses two fluorescent dyes that bind to nucleic acids: green-fluorescent SYTO 9 and red-fluorescent propidium iodide (PI). The cell-permeant SYTO 9 stains all live cells while the non-permeant PI stains nucleic acids only in cells with damaged membranes. Following incubation with the cells, the SYTO 9 and PI probes are excited at 485 nm and emit at 528 nm and 638 nm respectively. The live/dead cells ratio values are derived from the ratio between the background-subtracted red and green fluorescence intensities. Figure 5b shows the normalized live/dead cells ratio values of *Shewanella oneidensis* MR-1 when exposed to InSe-EGCG nanosheets and nanoparticles at concentrations ranging from 0 to 62.5 mg/L. Similar to GBV assays, all dilutions were done with 5 mM EGCG-water to keep the level of EGCG constant. The live/dead assays results are in agreement with the GBV assays and show no evidence of membrane disruption due to association of InSe-EGCG nanosheets or nanoparticles with bacterial cells. However, a control with free EGCG-water reduces the live/dead cells ratio which indicates bacterial death. The results of these assays confirm that the impact of InSe nanosheets on bacterial growth is low and that it is driven by free EGCG molecules and not by the InSe nanosheets.

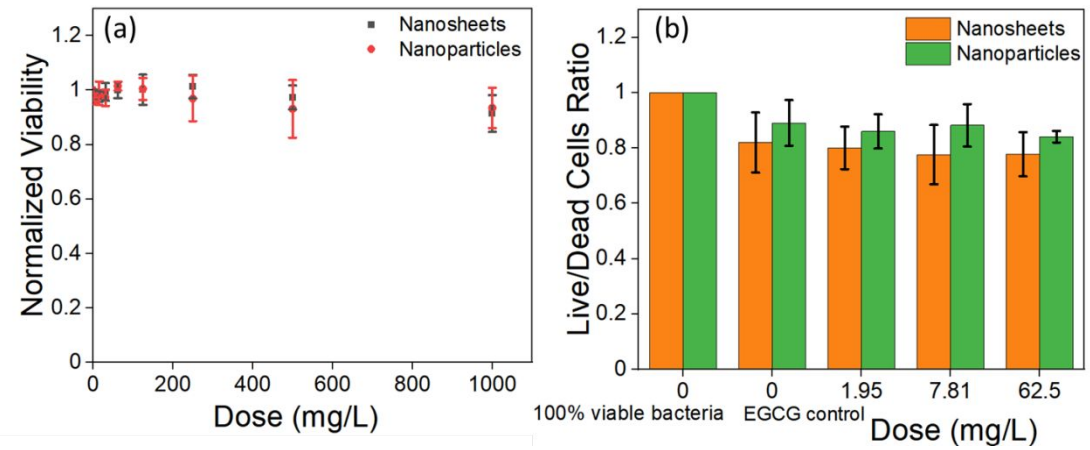

Figure 5 – (a) Normalized growth-based viability (GBV) assays results of InSe-EGCG nanosheets and nanoparticles (0-1000 mg/L), and (b) normalized live/dead cells ratio values of InSe-EGCG nanosheets and nanoparticles (0-62.5 mg/L) on *Shewanella oneidensis* MR-1. All dilutions of InSe-EGCG were done with 5mM EGCG-water. All the data were obtained in triplicate samples and averaged.

To confirm this conclusion and to understand the impact of adsorbed EGCG molecules on the InSe nanosheet on bacterial growth, we conducted time dependent bacterial growth assays of *Shewanella oneidensis* MR-1 cells when exposed to thoroughly washed InSe-EGCG nanosheets. While these conditions do not represent a realistic environmental scenario, they still provide an important insight about the impact of the EGCG adsorbates on bacterial cells' growth. Figure 6 shows the optical density of the bacterial cultures at 600 nm (OD 600) as a function of time for bacterial cells that were exposed to washed InSe-EGCG nanosheets at increasing concentrations.

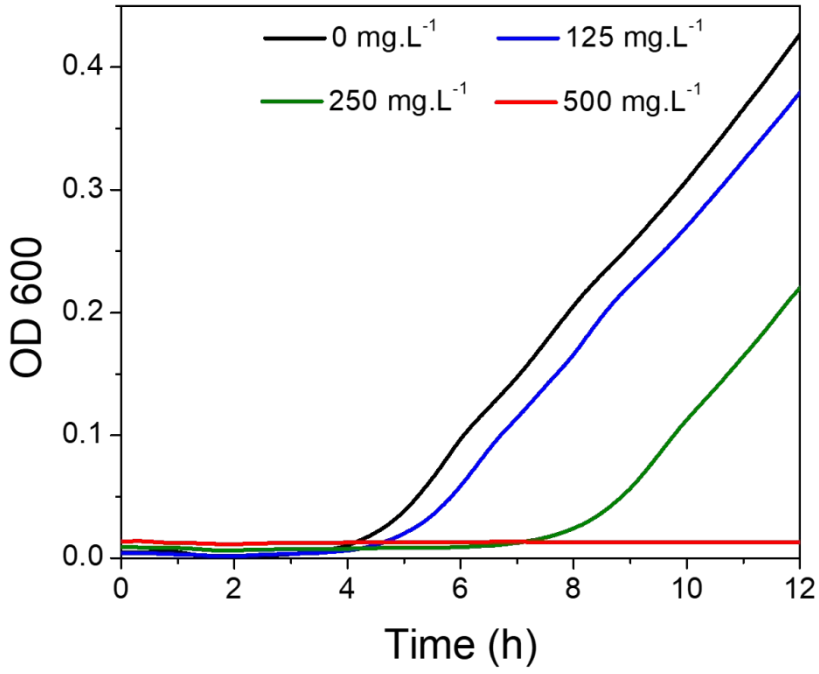

Figure 6– Growth curves of *Shewanella oneidensis* MR-1 bacterial cells at varying concentrations of thoroughly washed InSe-EGCG nanosheets. The optical density at 600 nm (OD 600) decreases with decreased bacterial growth.

The optical density of bacterial growth solutions (OD 600) is proportional to the density of bacterial cells in the solution. Following a typical lag time of four hours, the bacterial cells enter an exponential growth phase, leading to an increase in optical density. A clear InSe-EGCG concentration dependent decrease in bacterial growth and viability is observed. As mentioned previously, this growth inhibition is attributed to the impact of EGCG, either when adsorbed to the nanosheet surface or when desorbed from the nanosheets when the nanosheets interact with the cells. While the impact on cell growth is clear, it should be noted that the impact of InSe-EGCG on *Shewanella oneidensis* MR-1 is low compared to other nanomaterials studied in the past. For example, a similar impact on *Shewanella oneidensis* MR-1 cell growth was observed when exposed to a 500-fold lower concentration of CdSe quantum dots.[22]

SUMMARY AND CONCLUSIONS

2D materials have become a major focus in materials chemistry research due to their unique morphology and properties. InSe nanosheets are emerging 2D nanomaterials with significant applicability in flexible and wearable electronic devices. A semi bottom-up synthesis method enables producing scalable mg quantities of hydrophobic InSe nanosheets or 2D materials, which are not soluble in aqueous media. Our studies show that the hydrophobic InSe nanosheets can be colloidally stabilized in aqueous media by coating their surface with an amphiphilic natural organic matter (NOM) simulant molecule, epigallocatechin gallate (EGCG) via physisorption, with the best colloidal stabilization efficiency of 1 mg/ml InSe nanosheets at EGCG concentrations greater than 0.75 mM. Bacterial exposure studies with the water-soluble EGCG surface-modified InSe (InSe-EGCG) nanosheets and nanoparticles, which were conducted using *Shewanella oneidensis* MR-1, show that the toxicity of InSe-EGCG nanosheets and nanoparticles is driven by the EGCG ligands and not by InSe. No measurable ROS levels are observed when the nanosheets are illuminated with ambient room light. This suggests that the EGCG coating may inhibit the formation of ROS from the InSe semiconducting material. Our results show that the impact of InSe-EGCG nanosheets on bacterial growth of *Shewanella oneidensis* MR-1 is driven by the EGCG ligand molecules either when they are conjugated to the nanosheet surface or when they desorb from the nanosheets and interact with the bacterial cells. While there have been some reports on the adverse impact of EGCG on bacterial cells, more systematic studies are needed to understand the mechanism of interaction between EGCG and bacterial cells at the molecular level. It is possible that association of EGCG molecules, through their multiple hydroxyl groups with the bacterial cell membrane, or permeation of EGCG molecules into the cells, induce oxidative stress, which adversely impact cell growth. In this scenario, the InSe nanosheets act as a delivery vector by adsorbing EGCG molecules onto their surface and interacting with the cells. The EGCG-coated InSe nanosheets likely amplify the impact of EGCG on bacterial cell growth due to an increased local concentration of EGCG at the vicinity of the cells. It should be noted however, that the overall impact of InSe-EGCG nanosheets on the growth and viability of *Shewanella oneidensis* MR-1 cells is low compared to the impact of other synthetic nanoparticles like CdSe quantum dots which we previously studied. The study highlights a significant environmental concern due to the broad distribution of chemically stable, hydrophobic nanosheets in electronic devices and their release to the environment when discarded post use. While 2D materials like InSe are minimally toxic, they are expected to

aggregate and settle in the soil due to their hydrophobicity and the lack of an obvious biodegradation pathway. It is therefore possible, even likely, that the nanosheets will be solubilized by natural organic matter (NOM) or other contaminants. The surface transformation of the nanosheets will bring them into aqueous systems where they would interact with living organisms and impact them. The impact would be low or high depending on the ligand that colloidally stabilizes the nanosheets. While the ligand we chose for this study, EGCG, appears to induce low but measurable toxicity of InSe-EGCG nanosheets, other surfactants, for example dodecyltrimethylammonium bromide (DTAB) could lead to higher toxicity. The attention of the materials chemistry community should be devoted to develop effective recycling strategies and/or effective degradation pathways for 2D materials like InSe to mitigate the risk their use poses to the environment.

CONFLICTS OF INTEREST

The authors have no conflicts of interest to declare.

ACKNOWLEDGEMENTS

This work was supported by the National Science Foundation under Grant No. CHE-2001611, the NSF Centers for Sustainable Nanotechnology (CSN). The CSN is part of the NSF Center for Chemical Innovation Program. Sengupta's Doctoral research is partially supported by NIH Chemistry-Biology Interface (CBI) training grant NIH/NIGMS T32 GM066706. The authors thank Alessandra G. Gavin of the Department of Chemistry at the University of Minnesota for her support with bacterial live/dead assays. The authors thank the Howard Hughes Medical Institute (HHMI) Science Education Alliance (SEA) laboratory at UMBC for support with bacterial growth studies. The authors wish to acknowledge the invaluable advice of Joel Pedersen on the selection and use of natural organic matter simulants in this project.

REFERENCES

(1) Z. Wang, W. Zhu, Y. Qiu, X. Yi, A. von dem Bussche, A. Kane, H. Gao, K. Koski and R. Hurt, Biological and Environmental Interactions of Emerging Two-dimensional Nanomaterials, *Chem. Soc. Rev.*, 2016, **45**, 1750-1780.

(2) N. Valeria, C. Manish, G. K. Mercouri, S. S. Michael and C. N. Jonathan, Liquid Exfoliation of Layered Materials, *Science*, 2013, **340**, 1226419.

(3) G. Cunningham, M. Lotya, C. S. Cucinotta, S. Sanvito, S. D. Bergin, R. Menzel, M. S. P. Shaffer and J. N. Coleman, Solvent Exfoliation of Transition Metal Dichalcogenides: Dispersibility of Exfoliated Nanosheets Varies Only Weakly Between Compounds, *ACS Nano*, 2012, **6** (4), 3468-3480.

(4) I. U. Vakarelski, C. E. McNamee and K. Higashitani, Deposition of Silica Nanoparticles on a Gold Surface Via a Self-Assembled Monolayer of (3-mercaptopropyl)trimethoxysilane, *Colloids and Surfaces A: Physicochemical and Engineering Aspects*, 2007, **295** (1), 16-20.

(5) X. Yin, Y. Li, W. Wu, G. Chu, Y. Luo and H. Meng, Preparation of Two-Dimensional Molybdenum Disulfide Nanosheets by High-Gravity Technology, *Ind. Eng. Chem. Res.*, 2017, **56** (16), 4736-4742.

(6) Y. X. Huang, X. C. Dong, Y. M. Shi, C. M. Li, L. J. Li and P. Chen, Nanoelectronic Biosensors Based on CVD Grown Graphene, *Nanoscale*, 2010, **2** (8), 1485-1488.

(7) K. Kalantar-zadeh and J. Z. Ou, Biosensors Based on Two-Dimensional MoS_2, *ACS Sens.*, 2016, **1** (1), 5-16.

(8) J. Sun, H. Zhang, L. H. Guo and L. X. Zhao, Two-Dimensional Interface Engineering of a Titania-Graphene Nanosheet Composite for Improved Photocatalytic Activity, *ACS Appl. Mater. Interfaces*, 2013, **5** (24), 13035-13041.

(9) X. Y. Ji, L. L. Ge, C. Liu, Z. M. Tang, Y. F. Xiao, W. Chen, Z. Y. Lei, W. Gao, S. Blake, D. B. De, *et al.*, Capturing Functional Two-Dimensional Nanosheets From Sandwich-Structure Vermiculite for Cancer Theranostics, *Nature Communications,* 2021, **12** (1).

(10) T. Q. Wang, M. Z. Sun, H. L. Sun, J. Shang and P. K. Wong, Efficient Z-Scheme Visible-Light-Driven Photocatalytic Bacterial Inactivation by Hierarchical MoS_2-Encapsulated Hydrothermal Carbonation Carbon Core-Shell Nanospheres, *Appl. Surf. Sci.*, 2019, **464**, 43-52.

(11) Z. H. Miao, L. X. Fan, X. L. Xie, Y. Ma, J. Z. Xue, T. He and Z. B. Zha, Liquid Exfoliation of Atomically Thin Antimony Selenide as an Efficient Two-Dimensional Antibacterial Nanoagent, *ACS Appl. Mater. Interfaces*, 2019, **11** (30), 26664-26673.

(12) C. Moore, D. Movia, R. J. Smith, D. Hanlon, F. Lebre, E. C. Lavelle, H. L. Byrne, J. N. Coleman, Y. Volkov and J. McIntyre, Industrial Grade 2D Molybdenum Disulphide (MoS_2): An In-Vitro Exploration of the Impact on Cellular Uptake, Cytotoxicity, and Inflammation, *2D Mater.*, 2017, **4** (2), 025065.

(13) N. Balakrishnan, E. D. Steer, E. F. Smith, Z. R. Kudrynskyi, Z. D. Kovalyuk, L. Eaves, A. Patane and P. H. Beton, Epitaxial Growth of Gamma-InSe and Alpha, Beta, and Gamma-In_2Se_3 on Epsilon-GaSe, *2D Mater.*, 2018, **5** (3).

(14) G. W. Mudd, S. A. Svatek, T. Ren, A. Patane, O. Makarovsky, L. Eaves, P. H. Beton, Z. D. Kovalyuk, G. V. Lashkarev, Z. R. Kudrynskyi, *et al*., Tuning the Bandgap of Exfoliated InSe Nanosheets by Quantum Confinement, *Adv. Mater.*, 2013, **25** (40), 5714-5718.

(15) M. Brotons-Gisbert, D. Andres-Peuares, J. Suh, F. Hidalgo, R. Abargues, P. J. Rodriguez-Canto, A. Segura, A. Cros, G. Tobias, E. Canadell, *et al.*, Nanotexturing To Enhance Photoluminescent Response of Atomically Thin Indium Selenide with Highly Tunable Band Gap, *Nano Lett.*, 2016, **16**, 3221-3229.

(16) D. W. Boukhvalov, B. Gurbulak, S. Duman, L. Wang, A. Politano, L. S. Caputi, G. Chiarello and A. Cupolillo, The Advent of Indium Selenide: Synthesis, Electronic Properties, Ambient Stability and Applications, *Nanomaterials*, 2017, **7** (11), 16, Review.

(17) W. Feng, J-B Wu, X. Li, W. Zheng, X. Zhou, K. Xiao, W. Cao, B. Yang, J-C Idrobo and L. Basile, Ultrahigh Photo-responsivity and Detectivity in Multilayer InSe Nanosheets Phototransistors with Broadband Response, *J. Mater. Chem. C*, 2015, **3** (27), 7022-7028.

(18) G. W. Mudd, S. A. Svatek, L. Hague, O. Makarovsky, Z. R. Kudrynskyi, C. J. Mellor, P. H. Beton, L. Eaves, K. S. Novoselov, Z. D. Kovalyuk, *et al.*, High Broad-Band Photoresponsivity of Mechanically Formed InSe-Graphene Van der Waals Heterostructures. *Adv. Mater.*, 2015, **27** (25), 3760-3766.

(19) W. Feng, F. L. Qin, M. M. Yu, F. Gao, M. J. Dai, Y. X. Hu, L. F. Wang, J. Hou, B. Li and P. A. Hu, Synthesis of Superlattice InSe Nanosheets with Enhanced Electronic and Optoelectronic Performance, *ACS Appl. Mater. Interfaces*, 2019, **11** (20), 18511-18516.

(20) N. Malhotra, O. B. Villaflores, G. Audira, P. Siregar, J. S. Lee, T. R. Ger and C. D. Hsiao, Toxicity Studies on Graphene-Based Nanomaterials in Aquatic Organisms: Current Understanding, *Molecules*, 2020, **25** (16).

(21) Udayabhanu, V. Pavitra, S. C. Sharma and G. Nagaraju, Epigallocatechin gallate (EGCG)-Assisted Combustion Synthesis of V_2O_5 Nanoparticles for Li-ion battery, *Ionics*, 2020, **26** (3), 1203-1210.

(22) D. N. Williams, S. Pramanik, R. P. Brown, B. Zhi, E. McIntire, N. V. Hudson-Smith, C. L. Haynes and Z. Rosenzweig, Adverse Interactions of Luminescent Semiconductor Quantum Dots with Liposomes and *Shewanella oneidensis*, *ACS Appl. Nano Mater.*, 2018, **1** (9), 4788-4800.

(23) M. A. Airo, S. Gqoba, M. P. Kalenga, S. Govindraju, M. J. Moloto and N. Moloto, Synthesis and Characterization of Indium Monoselenide Nanosheets: A Proposed Pseudo Top-Down Mechanism, *Journal of Crystal Growth*, 2014, **406**, 1-7.

(24) T. A. Qiu, T. H. T. Nguyen, N. V. Hudson-Smith, P. L. Clement, D. C. Forester, H. Frew, M. N. Hang, C. J. Murphy, R. J. Hamers, Z. V. Feng, *et al.*, Growth-Based Bacterial Viability Assay for Interference-Free and High-Throughput Toxicity Screening of Nanomaterials, *Analytical Chemistry*, 2017, **89** (3), 2057-2064.

(25) A. C. Mensch, R. T. Hernandez, J. E. Kuether, M. D. Torelli, Z. V. Feng, R. J. Hamers and J. A. Pedersen, Natural Organic Matter Concentration Impacts the Interaction of Functionalized Diamond Nanoparticles with Model and Actual Bacterial Membranes, *Environ. Sci. Technol.*, 2017, **51** (19), 11075-11084.

(26) G. Enlai, L. Shao-Zhen, Q. Zhao, M. J. Buehler, F. Xi-Qiao and X. Zhiping, Mechanical Exfoliation of Two-Dimensional Materials, *J. Mech. Phys. Solids*, 2018, **115**, 248-262.

(27) P. Marvan, V. Mazanek and Z. Sofer, Shear-Force Exfoliation of Indium and Gallium Chalcogenides for Selective Gas Sensing Applications, *Nanoscale*, 2019, **11** (10), 4310-4317.

(28) J. Kang, S. A. Wells, V. K. Sangwan, D. Lam, X. L. Liu, L. X. Jan, Z. Sofer and M. C. Hersam, Solution-Based Processing of Optoelectronically Active Indium Selenide, *Adv. Mater.*, 2018, **30** (38).

(29) R. P. Brown, M. J. Gallagher, D. H. Fairbrother and Z. Rosenzweig, Synthesis and Degradation of Cadmium-Free InP and InPZn/ZnS Quantum Dots in Solution, *Langmuir*, 2018, **34** (46), 13924-13934.

(30) K. H. Park, K. Jang, S. Kim, H. J. Kim and S. U. Son, Phase-Controlled One-Dimensional Shape Evolution of InSe Nanocrystals, *J. Am. Chem. Soc.*, 2006, **128** (46), 14780-14781.

(31) M. Isik and N. M. Gasanly, Temperature-Tuned Band Gap Characteristics of InSe Layered Semiconductor Single Crystals, *Mater. Sci. Semicond. Process.*, 2020, **107**, 104862.

(32) M. Airo, S. Gqoba, F. Otieno, M. Moloto and N. Moloto, Structural Modification and Band-Gap Crossover in Indium Selenide Nanosheets, *RSC Adv.*, 2016, **6**, 40777.

(33) C. D. Wagner, W. M. Riggs, L. E. Davis, J. F. Moulder and G. E. Muilenberg, Handbook of X-Ray Photoelectron Spectroscopy, Perkin-Elmer Corporation, Physical Electronics Division, Eden Prairie, Minn., 1979, 55344.

(34) D. Cahen, P. J. Ireland, L. L. Kazmerski and F. A. Thiel, X-Ray Photoelectron and Auger Electron Spectroscopic Analysis of Surface Treatments and Electrochemical Decomposition of $CuInSe_2$ Photoelectrodes, *J. Appl. Phys.*, 1985, **57**, 4761-4771.

(35) D. W. Ma, W. W. Ju, Y. A. Tang and Y. Chen, First-Principles Study of the Small Molecule Adsorption on the InSe Monolayer, *Appl. Surf. Sci.,* 2017, **426**, 244-252.

(36) P. W. Taylor, M. T. J. Hamilton-Miller and P. D. Stapleton, Antimicrobial Properties of Green Tea Catechins, *Food Sci. Technol. Bull.*, 2005, **2**, 71-81.

(37) X. Y. Wang, H. Y. Nan, W. Dai, Q. Lin, Z. Liu, X. F. Gu, Z. H. Ni and S. Q. Xiao, Optical Studies of the Thermal Stability of InSe Nanosheets, *Appl. Surf. Sci.*, 2019, **467**, 860-867.

(38) M. K. Gari, P. Lemke, K. H. Lu, E. D. Laudadio, A. H. Henke, C. M. Green, T. Pho, K. N. L. Hoang, C. J. Murphy, R. J. Hamers and Z. V. Feng, Dynamic Aqueous Transformations of Lithium Cobalt Oxide Nanoparticle Induce Distinct Oxidative Stress Responses of *B. subtilis*., *Environ. Sci.: Nano*, 2021, **8** (6), 1614-1627.

(39) D. Sharan, D. Wolfson, C. M. Green, P. Lemke, A. G. Gavin, R. J. Hamers, Z. V. Feng, and E. E. Carlson, Chronic Exposure to Complex Metal Oxide Nanomaterials Induces Production of Reactive Oxygen Species in Bacteria, *Environ. Sci.: Nano*, 2023, Advance Article.